

Oriental Medicine

Preparation and characterization of resistant starch type 3 from yam and its effect on the gut microbiota

Xue-Qian Zhang1, Di Liang1, Na Liu1, Ou Qiao1, Xue-Min Zhang2, Wen-Yuan Gao1, Xia Li1*

¹Tianjin Key Laboratory for Modern Drug Delivery & High-Efficiency, School of Pharmaceutical Science and Technology, Tianjin University, Tianjin 300193, China. ²Key Laboratory of Modern Chinese Medicine Resources Research Enterprises, Tianjin 300410, China.

*Corresponding to: Xia Li. Tianjin Key Laboratory for Modern Drug Delivery & High-Efficiency, School of Pharmaceutical Science and Technology, No. 92, Weijin Road, Nankai District, Tianjin 300193, China. E-mail: lixia2008@tju.edu.cn.

Author contributions

Xue-Qian Zhang, conceptualization, methodology, writing – original draft, formal analysis, data curation. Di Liang, methodology, software, data curation. Na Liu, methodology, software. Ou Qiao, software, writing – review. Xue-Min Zhang, methodology, software. Wen-Yuan Gao, resources, project administration. Xia Li, conceptualization, writing – review & editing, funding acquisition.

Competing interests

The authors declare no conflicts of interest.

Acknowledgments

This work was supported by the key project at central government level (No. 2060302), Key R & D Project of Hebei Province (V1584581541757), the Science and Technology Project of Qinghai Province (No. 2021-SF-150) and the National Key R&D Program of China (No. 2019YFC1710603, No. 2019YFC1710604). We thank Austin Schultz (Edanz Group Ltd.), for editing the English text of a draft of this manuscript.

Abbreviations

RS, resistant starch; SCFAs, short chain fatty acids; ARYRS, autoclaving-retrogradation yam resistant starch; PDYRS, pullulanase debranching yam resistant starch; WBC, water-binding capacity; SOL, solubility; SP, swelling power; SW, swollen mass; FT-IR, Fourier transform infrared spectroscopy; YS, yam starch.

Peer review information

Traditional Medicine Research thanks Vinay Sridhar and other anonymous reviewers for their contribution to the peer review of this paper.

Citation

Zhang XQ, Liang D, Liu N, et al. Preparation and characterization of resistant starch type 3 from yam and its effect on the gut microbiota. *Tradit Med Res.* 2022;7(2):11. doi: 10.53388/TMR20211011247.

Executive editor: Rui-Wang Zhao.

Received: 15 April 2021; **Accepted:** 27 July 2021; **Available online:** 10 January 2022.

© 2022 By Author(s). Published by TMR Publishing Group Limited. This is an open access article under the CC-BY license. (http://creativecommons.org/licenses/BY/4.0/).

Abstract

Background: Yam (Dioscorea opposita Thunb.) has been consumed as a food and used in traditional Chinese medicine for thousands of years, Resistant starch (RS) 3 is of particular interest because it is heat-resistant, safe and non-toxic, and retains good nutritional benefits; it is therefore used in a wide range of traditional and emerging foods as a heat-stable prebiotic ingredient. In our previous study, we found that yam RS includes strong lipid-lowering and anti-constipation activities. Methods: Yam RS3 was prepared by autoclaving-retrogradation and pullulanase debranching to yield autoclaving-retrogradation yam RS and pullulanase debranching yam RS, respectively. First, the physicochemical properties of both RS3s were analyzed. Second, the structures of the RS3s were characterized by scanning electron microscopy, X-ray powder diffraction, and Fourier transform infrared spectroscopy. Finally, the regulatory effects of the RS3s on the gut microbiota were evaluated using an in vitro fecal fermentation model. Results: The RS content of the RS3s decreased after processing, but was higher in pullulanase debranching yam RS (35.67%) than in autoclaving-retrogradation yam RS (28.71%). Compared with native yam starch, RS3s lost their original granular shapes and instead exhibited irregularly shapes with continuous phases. The crystalline structure of the RS3s was completely altered, with pullulanase debranching yam RS exhibiting B-type patterns. Both RS3s, and especially pullulanase debranching yam RS, promoted a significant increase in short chain fatty acid content after in vitro fermentation (all P < 0.05). Moreover, pullulanase debranching yam RS significantly increased the abundance of beneficial bacteria and decreased the abundance of harmful bacteria such as *Escherichia* and *Shigella* (all P < 0.05). Conclusion: Our findings show that yam RS3s can regulate the composition of the gut microbiota and promote the production of short chain fatty acid, especially butyric acid. Pullulanase debranching was a more effective method for producing functional yam RS3.

Keywords: Yam; resistant starch type 3; physicochemical properties; short chain fatty acids; gut microbiota







Yam(medicinal site)



Yam starch

Highlights

This study finds that Yam (*Dioscorea opposita* Thunb.) resistant starch 3 can regulate the composition of the gut microbiota and promote the production of short chain fatty acid.

Tradition

Yam (*Dioscorea opposita* Thunb.) is one of the earliest known and most used ingredients in traditional Chinese medicine. The first mention of yam as a medicinal ingredient is in *Shennong's Classic of Materia Medica*, which was written during the Eastern Han Dynasty (25 C.E.–220 C.E.) and listed yam as a top-grade therapeutic substance. In *Compendium of Materia Medica* (written between 1552 C.E. and 1578 C.E.), Li Shizhen (born in 1578 C.E.) stated that yam can strengthen the spleen and stomach (therapeutic effects that are similar to regulation of gastrointestinal functions in Western medicine).

Background

Yam, the dry root of Dioscorea opposita Thunb. (Figure 1), has been used in traditional Chinese medicine for thousands of years as a nutritious food source and tonic. Chinese yam has been cultivated since the Xia (2070 to 1600 B.C.E.) and Shang (1600 to 1046 B.C.E.) dynasties of China, and gradually came to be used as a medicinal material during the Ming (1368 to 1644 C.E.) and Qing (1636 to 1911 C.E.) dynasties of China [1]. Yam was first mentioned in Shennong's Classic of Materia Medica, which was written during the Eastern Han Dynasty (25-220 C.E.) and listed yam as a top-grade therapeutic substance [2]. This book is the earliest known Chinese pharmaceutical text. There is also historical evidence that many Chinese medical scientists used yam, such as Li Shizhen (born in 1578 C.E.), who wrote Compendium of Materia Medica (written in 1552 to 1578 C.E.) and Zhang Zhongjing (born about 150-154 C.E.), who wrote Synopsis of Golden Chamber (published in the 3rd century C.E.), both of whom emphasized the role of yams in strengthening the spleen and stomach (it is similar to regulating gastrointestinal function in Western medicine) [3]. Modern studies have shown that yam is rich in fiber and enzymes and can be used to help regulate gastrointestinal functions, such as in the treatment of chronic gastroenteritis, protection of the gastric mucosa, and regulation of intestinal flora [4, 5]. While there are numerous active ingredients in yam, starch is one of the main components, accounting for 20%-60% of the total biomass of the tuber [6]. Yam is a main component of many patented Chinese medicines, such as Liuwei Dihuang pills (SFDA in China approval No. Z34020130), Qiwei Duqi pliis (SFDA in China approval No. Z33020157), and Wubi Shanyao pills (SFDA in China approval No. Z33020111). It is used as medicine in the form of a powder, in which starch plays a very important role. The structure and activity of starch changes during the processing of whole yam, and some resistant starch (RS) is produced. Bioactive carbohydrates, including RS and polysaccharides, have a variety of health benefits in humans [7]. However, these starches are often discarded in the process of isolating bioactive compounds. In addition, native starches do not consistently withstand extreme processing conditions, such as high shear rates, high temperatures, strong acid and alkali treatments, and freeze-thaw cycles, which limits their use in many industries [8]. Therefore, different methods are usually used to modify native starch to expand its applications.

RS is a newly identified type of dietary fiber that cannot be degraded by digestive enzymes in the human stomach and small intestine but can be fermented by the gut microbiota in the colon to produce short chain fatty acids (SCFAs), thereby promoting the growth of functional colonic microorganisms and playing such roles as preventing colon cancer, improving insulin resistance, and lowering blood lipid levels [9, 10]. Generally, RSs can be classified into five categories: RS1, RS2, RS3, RS4, and RS5 [11]. RS3 in particular has

aroused widespread interest because it is highly heat-stable and retains its nutritional qualities even after heating. In addition, its properties include a white color, no distinctive smell, low water absorption, and a delicate taste [12], making it a candidate for a wide range of applications in the food and pharmaceutical industries.

The processing conditions used in the preparation of RS3 have a substantial influence on its structural characteristics. RS3 is formed by recrystallization of gelatinized starch during cooling. Autoclaving can fully gelatinize starch granules and cause complete release of amylose molecules, thus promoting full combination between amylose molecule double helices and facilitating the formation of RS [11]. This was the earliest method used to prepare RS. The number of autoclaving-cooling cycles used in this process has a significant impact on the formation of RS3 [13]. Starch retrogradation is mainly caused by amylose molecule interactions because it is easy to form hydrogen bonds between amylose. Enzymatic debranching is often used to generate more amylose, so as to further promote the formation of RS3. Compared with pure amylose, which is more expensive to produce and more difficult to dissolve in water, this method is more suitable for large-scale production of RS3. Pullulanase, which can selectively cleave 1, $6\text{-}\alpha\text{-}D\text{-}glucosidic}$ bonds, is commonly used as a debranching enzyme in this context [14]. Currently, the autoclaving method is typically combined with the enzymatic debranching method to increase RS3 vield.

In our previous studies, we found that native yam starch (YS) has good anti-digestibility [15], and that yam RS properties include anti-constipation and blood lipid-lowering activities [16]. Accordingly, the aim of this study was to compare the physicochemical properties, structural characteristics, and gut microbiota regulatory activity of two kinds of yam RS3, so as to provide a basis for the development of traditional Chinese medicines based on yam.

Materials and methods

Materials and reagents

Chinese yam (*Dioscorea opposite* Thunb.) was obtained from Wenxian County, Jiaozuo City, Henan Province, and authenticated by Prof. Wenyuan Gao, Tianjin University, China. Pullulanase (1,000 ASPU/mL) and porcine pancreatic alpha-amylase (12 U/mg) were purchased from Yuanye Biological Technology Co. (Shanghai, China). Amyloglucosidase (100,000 U/mL) was purchased from Macklin Biological Technology Co., Ltd. (Shanghai, China). Acetic acid, propionic acid, isobutyric acid, n-butyric acid, isovaleric acid, and n-valeric acid were purchased from Sigma-Aldrich Chemical Co. (St. Louis, MO, USA). All other chemicals used in the experiments were of analytical grade (Jiangtian Chemical Co., Ltd., Tianjin, China).



Figure 1 Yam whole plant, medicinal root, and starch

Isolation of YS

Starch was isolated from fresh yam according to the method described by Jiang et al. [17] with slight modifications. Fresh yams were washed, peeled, and cut into small pieces, which were then homogenized with a juicer and filtered through a 200-mesh sieve. The residue left on the sieve was washed several times with distilled water, then discarded, and the filtrate was allowed to stand for about 1–2 hours. Next, the supernatant was discarded, and the precipitate was washed with distilled water repeatedly until the supernatant was colorless. Then, the precipitate was washed repeatedly with 95% ethanol and centrifuged $(3,000 \times g, 10 \text{ min})$. The upper layer containing protein, fiber, and other substances lighter than starch was scraped off, and the lower layer containing impurities heavier than starch was also discarded. The starch was then dried at 50 °C for 24 hours, crushed, and passed through a 100-mesh sieve.

Preparation of RS

Autoclaving-retrogradation yam resistant starch (ARYRS). First, 9 g of YS was accurately weighed, and 30 mL water was added to obtain starch suspension. The suspension was gelatinized in an autoclave at 121 $^{\circ}$ C and 0.05 MPa for 30 min, and then cooled to room temperature. The gelatinized starch was cooled at 4 $^{\circ}$ C for 48 h, then dried at 50 $^{\circ}$ C for 24 h. Finally, the starch was ground and passed through a 100-mesh sieve for use.

Pullulanase debranching yam resistant starch (PDYRS). First, 9 g of starch was suspended in 30 mL deionized water and autoclaved at 121 °C and 0.05 MPa for 30 min. After cooling to 58 °C, the pH of the paste was adjusted to 4.7 with 0.5M HCl, after which the solution was debranched by pullulanase (40 ASPU/g) for 12 h. The starch was cooled to room temperature, further cooled at 4 °C for 48 h, dried at 50 °C for 24 h, crushed, passed through a 100-mesh sieve, and set aside for use.

Physicochemical properties

Moisture and protein. The protein content of the samples was determined according to the standard American Association of Cereal Chemists method [18]. Briefly, 1 g of starch was accurately weighed with low-nitrogen weighing paper. The sample was then transferred to a numbered Kjeldahl nitrogen tube (ZDDN-II, Zhejiang Top Yiqi Co., Ltd., Hangzhou, China) to measure the protein content. The moisture content of the samples was measured by oven drying and heating at 105 °C for 24 hours until a constant weight was reached [19].

RS content. The method described in Association of Official Analytical Chemists (2002) was used to measure the RS content [20]. Briefly, 0.1 g of each sample was added to 4 mL of mixed enzyme solution (porcine pancreatic α -amylase 10 mg/mL, amyloglucosidase 3 U/mL) and hydrolyzed at 37 °C for 16 h. The reaction was terminated by adding 4 mL 95% ethanol, followed by centrifugation at 10,000 g for 10 min. The precipitate was washed with 50% ethanol, then centrifuged again, and the process was repeated twice. The precipitate was dissolved in 2 mL KOH (2 M) solution, then 8 mL sodium acetate buffer solution (1.2 M, pH=3.8) and 0.1 mL amyloglucosidase (3,300 U/mL) were added, mixed and shaken in a water bath at 50 °C for 40 min. The glucose content was determined by the phenol sulfuric acid method.

Water-binding capacity (WBC). The WBC of the samples was assessed using the method described by Huang et al. [16] with some modification. First, 1 g of starch was mixed with 15 mL distilled water and stirred for 1 h. After centrifugation $(3,000 \times g, 10 \text{ min})$, the supernatant was carefully removed and drained for 10 min. The wet starch precipitate was then weighed.

Solubility (SOL) and swelling power (SP). SOL and SP were measured using the method described by Jiang et al. [15] with a slight modification. First, 2% starch suspensions (w/v) were heated in a water bath at 65, 75, 85, or 95 °C for 1 h and stirred continuously. The cooled suspensions were then centrifuged for 10 min (3,000 \times g). After centrifugation, the supernatant was slowly poured into an evaporating pan, dried at 105 °C, and weighed. The lower sediment was directly weighed to obtain the swollen mass (SW). SOL and SP

were calculated as follows:

SOL (%) = Weight of dried supernatant \times 100 / Starch_{dwb} SP (g/g) = SW / (Starch_{dwb} \times (100% – SOL%)) where starch_{dwb} is the dry water basis starch weight.

Scanning electron microscopy

Field emission scanning electron microscopy (Apreo S LoVac, FEI, Czech Republic) was performed at an acceleration voltage of 20 kV to examine starch morphology. Prior to analysis, the starch samples were placed on double-sided adhesive tape attached to the metal tube and then coated with gold.

Fourier transform infrared spectroscopy (FT-IR)

The Fourier transform infrared spectra of starches were obtained by the potassium bromide (KBr) method using an infrared spectrometer (Tensor27, Bruker, Karlsruhe, Germany). The spectral range was 4,000–400 cm⁻¹, the resolution was 4 cm⁻¹, and each sample was scanned 32 times.

X-ray diffraction

A powder X-ray diffractometer (MIniflex600, Tokyo, Japan), operated at 40 kV and 15 mA, was used to observe the crystalline structure of the starches. The diffraction patterns were collected in the range of 5° –40° (20) with a speed of 4° (20)/min and a step size of 0.02° (20).

In vitro fecal fermentation

In vitro human fecal fermentation of starches was performed as described previously [21, 22] with minor modifications. Fresh fecal samples were collected from three healthy donors (aged 22-35 years, two females, one male) who had not taken antibiotics or probiotics or had any gastrointestinal disorders within the preceding 3 months. Informed consent was obtained from each donor participating in this study. All experiments were completed within 2 hours of collecting the feces. First, 1 g of feces was added to 8 mL sterile phosphate buffered saline (0.1 mol/L, pH = 7.0) pre-reduced with 0.1% (w/v) cysteine hydrochloride, mixed evenly, and centrifuged at 4 $^{\circ}\text{C}$ for 5 min (500 g). The fecal supernatants from all three donors were combined in equal amounts for use as the fecal inoculum. Next, 100 mg of starch was added to a fermentation tube containing 5 mL of fermentation medium and 2 mL of fecal inoculum and anaerobically cultured at 37 °C for 24 h. A tube containing fermentation medium and fecal inoculum only was used as the blank control. After the fermentation, the samples were centrifuged at 14,000 ×g for 20 min, and the supernatant and precipitate were stored at $-80~^{\circ}\text{C}$ until analysis.

Determination of SCFAs

SCFA contents were determined using a gas chromatograph-mass spectrometer (TRACE_1300GC-ISQ_LT, Thermo Co., Ltd., Waltham, MA, USA) equipped with a TG WAX column (30 m \times 0.25 mm \times 0.25 μm). First, 0.1 g of fermentation liquid was added to 2 mL of a 10% phosphoric acid aqueous solution and mixed well, followed by extraction with 2 mL ether for 5 min and centrifugation at 3,000 ×g for 15 min. After centrifugation, the ether phase was removed, then the extraction was performed twice more using 1 mL ether and the same procedure, after which all three extracts were combined. The entire volume of the ether extract was fixed, and the sample was injected for analysis. The acetic acid, propionic acid, isobutyric acid, n-butyric acid, isovaleric acid, and n-valeric acid contents were determined using the standard curve method. The detection conditions were as follows: column temperature: 100 °C (5 min), -5 °C/min, -150 °C (10 min), -30 °C/min, -240 °C (30 min); flow rate: 1 mL/min; split ratio: 75:1; carrier gas: helium; injector: 240 °C; electron ionization source bombardment voltage: 70 ev; single ion scanning mode: quantitative ion 60, 73; ion source temperature: 200 °C; connecting wire temperature: 250 °C.

DNA extraction and MiSeq sequencing

The TruSeqTM DNA Sample Prep kit (Illumina Inc., San Diego, CA,

USA) was used to extract genomic DNA from fermentation samples. Amplification of the 16S rRNA V3-V4 hypervariable region was performed with universal primers: 338F (5'-ACTCCTACGGGAGGCAGCAG-3'), and 806R (5'-GGACTACHVGGGTWTCTAAT-3'). All polymerase chain reactions were performed on a thermocycler polymerase chain reaction system (ABI GeneAmp 9700, Waltham, MA, USA). Polymerase chain reaction products were detected using a 2% agarose gel and purified with a AxyPrep DNA Gel Extraction kit (Axygen Biosciences, Union City, CA, USA). The purified amplicons were quantified using a QuantiFluor-ST blue fluorescence quantification system (Promega, Madison, GA, USA) and sequenced on an MiSeq platform (IIIumina, San Diego, CA, USA) according to standard protocols by the Shanghai MajorBio Bio-Pharm Technology Co., Ltd. (Shanghai, China).

Statistical analysis

Data analysis was carried out using Origin 8.5 (Origin Lab Co., Ltd., Northampton, MA, USA). The statistical analysis was performed by one-way analysis of variance with Duncan's multiple range test using SPSS 19 software (IBM, Chicago, IL, USA). All results are presented as mean \pm standard error of mean from triplicate measurements.

Results

Moisture, protein, RS, and WBC

The physicochemical properties of YS and RS are shown in Table 1. YS and the two RSs exhibited moisture contents between 9.49% and 10.96%. Compared with the YS, the protein content of the RSs was significantly decreased, mainly because protein structure is destroyed by high-temperature processing. The RS content decreased from 42.34% in YS to 28.71% in ARYRS and 35.67% in PDYRS because of modifications caused by processing. However, the RS content of PDYRS was higher than that of ARYRS, indicating that pullulanase

promoted the formation of RS. The WBCs of ARYRS (263.8%) and PDYRS (125.81%) were higher than that of YS. It has been reported that increasing hydrophilic groups or decreasing hydrophobic tendencies during the modification process increases WBC [23].

SOL and SP

The SOL and SP of YS and the RSs at different temperatures are presented in Table 2 and Table 3, respectively. The SOL and SP of the samples increased gradually as the temperature increased. SOL increases with temperature because the crystal structure is gradually destroyed during the heating process, and the hydrogen bonds in water easily associate with the hydroxyl groups in amylose [24]. As shown in Table 2, ARYRS had the highest SOL, followed by PDYRS, and then YS. Starch granule SP reflects the degree of starch chain binding in the amorphous and crystalline domains. The swelling of starch particles starts from the relatively loose amorphous region and then proceeds to the crystalline region [1]. The two modified starches, especially ARYRS, exhibited better SP than native starch.

Scanning electron microscopy

The scanning electron microscopy micrographs of YS and the two RSs are shown in Figure 2. The granules of native YS were flat ovals, triangular ovals, or quasi-circles, and the surfaces were smooth and compact. These results are consistent with the granular shapes of YSs reported in the literature [16]. Compared with YS, the apparent morphology of the modified starches was noticeably different. As can be seen in Figure 2, the RS3 particles had lost their original granular shapes and exhibited an irregular block-like appearance. The particle size was significantly larger and presented a continuous phase. In addition, the surfaces of the RS granules were quite uneven and exhibited multiple layered strips (yellow arrows in Figure 2). Similar phenomena have been observed in cowpea starch [25] and lotus seed starch [24].

Table 1 Moisture, protein, RS, WBC, and relative crystallinity of YS and RSs

Sample	Moisture (%)	Protein (%)	RS (%)	WBC (%)	Relative crystallinity (%)
YS	10.96 ± 0.04^{a}	0.20 ± 0.03^{a}	42.34 ± 0.12^a	94.57 ± 0.31^a	35.14 ± 0.13^a
ARYRS	10.00 ± 0.01^{b}	0.05 ± 0.00^{b}	28.71 ± 0.27^{c}	263.80 ± 0.64^{b}	3.75 ± 0.03^{b}
PDYRS	$9.49 \pm 0.06^{\circ}$	$0.04 \pm 0.00^{\circ}$	35.67 ± 0.22^{b}	125.81 ± 1.06°	30.17 ± 0.21^{c}

RS, resistant starch; WBC, water-binding capacity; YS, yam starch; ARYRS, autoclaving-retrogradation yam resistant starch; PDYRS, pullulanase debranching yam resistant starch. Mean \pm standard error of mean, n = 3. Values with different letters in the same column are significantly different (P < 0.05).

Table 2 Effect of temperature on SOL of YS and RSs

Sample	65 °C	75 °C	85 °C	95 °C
YS	4.85 ± 0.09^{c}	$8.85 \pm 0.06^{\circ}$	$11.23 \pm 0.25^{\circ}$	$15.04 \pm 0.10^{\circ}$
ARYRS	7.46 ± 0.11^{b}	10.66 ± 0.11^{b}	12.45 ± 0.17^{b}	17.59 ± 0.38^{b}
PDYRS	34.24 ± 0.27^{a}	40.31 ± 0.18^{a}	52.06 ± 0.29^{a}	60.46 ± 0.31^{a}

RS, resistant starch; SOL, solubility; YS, yam starch; ARYRS, autoclaving-retrogradation yam resistant starch; PDYRS, pullulanase debranching yam resistant starch. Mean \pm standard error of mean, n = 3. Values with different letters in the same column are significantly different (P < 0.05).

Table 3 Effect of	temperature on	SP of YS and	RSs

Sample	65 °C	75 °C	85 °C	95 °C
YS	$2.12 \pm 0.01^{\circ}$	$3.58 \pm 0.03^{\circ}$	$4.52 \pm 0.08^{\circ}$	6.25 ± 0.11^{b}
ARYRS	8.79 ± 0.01^{a}	10.11 ± 0.00^{a}	10.24 ± 0.09^a	11.60 ± 0.20^{a}
PDYRS	5.36 ± 0.03^{b}	6.16 ± 0.02^{b}	$6.37 \pm 0.03^{\rm b}$	$7.34 \pm 0.06^{\circ}$

RS, resistant starch; SP, swelling power; YS, yam starch; ARYRS, autoclaving-retrogradation yam resistant starch; PDYRS, pullulanase debranching yam resistant starch. Mean \pm standard error of mean, n = 3. Values with different letters in the same column are significantly different (P < 0.05).

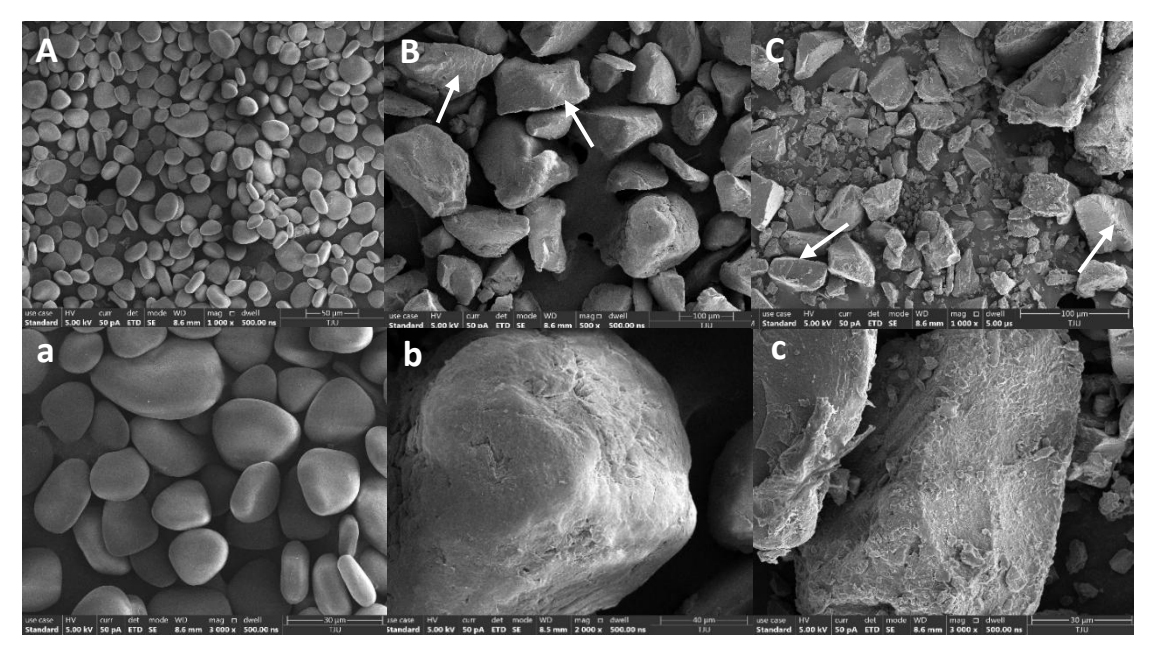


Figure 2 Scanning electron microscopy of YS and RSs. A, YS $1,000 \times$; a, YS $3,000 \times$; B, ARYRS $1,000 \times$; b, ARYRS $3,000 \times$; c, PDYRS $3,000 \times$. Yellow arrows, layered strips on the surface of the particles; YS, yam starch; ARYRS, autoclaving-retrogradation yam resistant starch; PDYRS, pullulanase debranching yam resistant starch; RS, resistant starch.

FT-IR

Infrared spectroscopy can analyze the molecular structure of starch granules based on short-range differences in infrared signal levels, and changes in peak intensity indicate changes in starch conformation [26]. All samples displayed absorption peaks at around 3,380 cm (-OH stretching vibration), 2,931 cm⁻¹ (-CH2 asymmetric stretching peak), 1,650 cm⁻¹ (stretching and bending vibration of the hydrogen-bonding -OH groups in water), 1,158 ${\rm cm}^{-1}$ (C-O and some C-O-H stretching vibration), 1,080 cm⁻¹ (C-O glycosidic bond stretching vibration), and 995 cm⁻¹ (vibration of C-O in alcohol hydroxyl group) (Figure 3) [6, 16]. Absorption from 800 cm⁻¹ to 1,200 cm⁻¹ reflects stretching vibration changes and hydration processing of C-C, C-OH, and C-H in the starch polymer configuration [27]. The absorption intensity in this region was weaker in the RS3s than in YS, indicating that the RS3s had undergone conformational changes. The absorption peak at 995 cm⁻¹ is related to the ordered structure of starch, and may reflect its relative crystallinity [28]. As Figure 3 shows, the crystallinity of the modified starch was reduced relative to that of YS. The modifications caused a broader absorption peak at 3,100 \mbox{cm}^{-1} to 3,400 $\mbox{cm}^{-1},$ indicating that the amylose chains formed more hydrogen bonds, creating complex vibrational stretching with hydroxyl groups [29]. Furthermore, ARYRS and PDYRS had a wider peak at 2,925 cm⁻¹ compared with YS, which was attributed to the retrogradation of amylose [30].

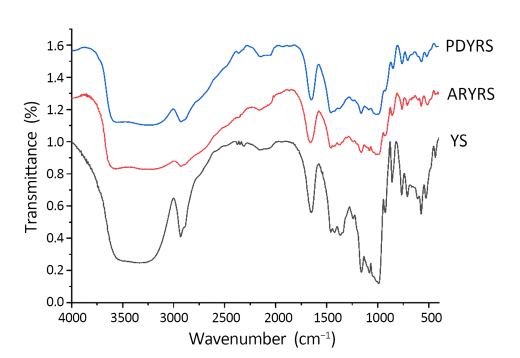


Figure 3 FT-IR of YS and RSs. RS, resistant starch; YS, yam starch; ARYRS, autoclaving-retrogradation yam resistant starch; PDYRS, pullulanase debranching yam resistant starch.

X-ray diffraction

The crystallinity and crystalline type of native YS and the RS3s were determined by X-ray diffraction. The results are presented in Supplementary Figure S1, and the corresponding parameters are shown in Table 1. The YS diffractogram showed three strong diffraction peaks at 15.18°, 17.12°, and 23.12° (20), indicating a C_A-type crystalline structure, as has been reported previously [31]. C-type starch is a mixture of A- and B-type unit cells [32]. The X-ray diffraction patterns of the modified starches were significantly different from that of YS. PDYRS exhibited a B-type crystallinity, as indicated by the single peak at $2\theta = 17.2^{\circ}$ and double peaks at $2\theta =$ 22.14° and 23.94°. The formation of the B-type crystallinity pattern was due to retrogradation at low temperature. In contrast, the crystalline structure of ARYRS was completely changed. There was only a single, weak peak at $2\theta = 17^{\circ}$ and a single broad peak at $2\theta =$ 22°. This change in crystallinity pattern was consistent with a previous report [33]. The crystallinity degrees calculated from the ratio of the diffraction peak areas and total diffraction areas were approximately 35.14%, 3.75%, and 30.17% for YS, ARYRS, and PDYRS, respectively.

SCFA production during in vitro fermentation

The average amounts of acetate, propionate, isobutyric acid, butyrate, isovaleric acid, and valeric acid produced during in vitro fecal fermentation are shown in Supplementary Table S1. The amounts of SCFAs produced by the two RS3s after anaerobic fermentation were significantly different, but acetic acid content was high for both. Compared with the blank control group, the acetic acid, propionic acid, isobutyric acid, butyric acid, isovaleric acid, and valeric acid contents of ARYRS and PDYRS after in vitro fecal fermentation were significantly increased, while the propionic acid content was decreased. A series of in vivo and in vitro experiments previously showed that RS can be used as a fermentation substrate to promote butyric acid production, while producing much less organic acid (such as lactic acid and succinic acid) [34]. Similarly, fermentation of yam RS3s produced a large amount of butyric acid. Compared with the blank control group (5.91 mg/kg), the butyric acid content in PDYRS was significantly higher, at 25.04 mg/kg, followed by ARYRS (10.35 mg/kg). It is worth noting that fermentation of PDYRS led to the production of more of each short-chain fatty acid than fermentation of ARYRS. These results clearly suggest that the different structural properties of the two RSs samples affected their fermentation

behavior.

Microbial composition during in vitro fermentation

Understanding the relationship among RS, gut microbiota, and bacterial metabolites is helpful for preventing disease and promoting health by regulating the gut microbiota. The effect of different vam RS3s on the gut microbiota composition was assessed by 16S rRNA gene sequencing (Supplementary Figure S2). At the phylum level (Supplementary Figure S2A), four types of bacteria were detected in all samples after in vitro fermentation, namely Firmicutes, Bacteroidota, Proteobacteria, and Actinobacteriota. Compared with the blank control group, in the PDYRS group there was a significant increase in the abundance of Firmicutes and Bacteroidota and a significant decrease in the abundance of Proteobacteria. The relative abundance of Bacteroides was decreased in the ARYRS group compared with the blank group, which may be related to the lower pH after fermentation. Xie et al. [35] and Wu et al. [36] made a similar observation. Notably, fermentation of ARYRS was associated with a higher proportion of Proteobacteria. This phenomenon may be attributable to the absorption of low molecular weight carbon sources by Proteobacteria such as Escherichia and Shigella to maintain their growth [37].

The microbiota composition shifts observed at the genus level are shown in Supplementary Figure S2B. To explore the main differences among the bacterial communities, the relative abundances of the top 20 genera were compared. For PDYRS, the relative abundance of the genera Bacteroides, Faecalibacterium, Enterococcus. Blautia. unclassified f Lachnospiraceae, Fusicatenibacter, Ruminococcus_torques_group, Eubacterium_eligens_group, and Alistipes was higher at the end of fermentation, whereas the abundance of Escherichia-Shigella, Phascolarctobacterium, Subdoligranulum, Collinsella, and Megamonas was reduced compared with the blank control group. The changes observed in most bacterial communities in the ARYRS group were opposite to those seen in the PDYRS group. Meanwhile, an increase in the relative abundance of Escherichia-Shigella was observed in the ARYRS group, similar to previous reports [38, 39]. Additionally, the ARYRS sample exhibited a lower relative abundance of Parasutterella than did the blank control group. A variety of animal models and human studies have shown that Parasutterella abundance is negatively correlated with high-fat diet induced metabolic phenotypes (including hypothalamic inflammation) [40]. These results suggest that supplementation of the fecal cultures with ARYRS and PDYRS changed the microbial composition in opposite ways, possibly because of differences in the fine structure of the RS3s.

Discussion

Modification of native YS significantly changes its physicochemical properties and structural characteristics. Compared with YS, the RS contents of both RS3s were lower. This might be due to overfragmentation of starch molecules, especially amylose, making them too small to integrate into the RS3 crystal structure [33]. The SOL, SW, and WBC are all related to the interaction between starch and water. The increased WBC observed in the RS3s may be related to degradation of amylopectin chains caused by autoclaving or pullulanase treatment, resulting in the formation of low molecular weight starch granules with high affinity for water molecules [41]. The increase in SOL may have occurred because the modification process greatly destroyed the crystalline region of native starch. SOL is used as an indicator of the degree of destruction of starch components [42]. Furthermore, SP is related to starch WBC: the higher the WBC, the greater the SP. In addition, granules with larger crystalline areas and stronger bonds in the crystalline regions swell less in cold water when subjected to heat [42]. The WBC results were consistent with the relative crystallinity results. In addition, the higher SOL of PDYRS than that of ARYRS can be attributed to the production of more amylose under the action of pullulanase, which was conducive to binding water molecules.

As can be seen from Figure 2, RS3 granules had a large, block-like

appearance with a continuous phase, which was attributed to the recrystallization of gelatinized starch [11, 43]. Nevertheless, the appearances of the two RS3s assessed in this study were similar, indicating that the different preparation methods used in this study had no significant effect on RS3 particle morphology. However, the long-range and short-range molecular orders of YS were greatly affected by autoclaving-retrogradation and pullulanase debranching. The FT-IR spectra (Figure 3) showed that all samples had similar characteristic peaks, and there were no changes between chemical groups, indicating that YS did not undergo chemical modification. However, the conformation of the starch changed, as shown by the differences in the width and strength of the absorption peaks among the samples. At the same time, the relative crystallinity of the RS3s decreased, as demonstrated by FT-IR and X-ray diffraction. The decrease in relative crystallinity after modification may be related to many factors, including crystal size, number of crystal regions, the orientation of the double helix in the crystal region, and the degree of double helix interaction [44]. Our results indicate that autoclaving can destroy the crystalline areas of starch, but that the use of pullulanase can alleviate this damage, leading to the formation of a new crystal structure.

The production of SCFAs, especially butyric acid, was significantly stimulated by both RS3s tested in this study. Butyrate plays an important role in human gut health by reducing inflammation, lowering the risk of colon cancer, and improving gut barrier function [45]. Studies have revealed that an impaired supply of butyric acid to colon cells can lead to intestinal shrinkage and impaired function, including a reduced immune response. In contrast, enhanced butyric acid supply to colon cells induces intestinal epithelial cell growth and intestinal cell differentiation and improves immune surveillance [46]. In normal cells, butyrate has been shown to induce proliferation at the crypt base, promoting healthy tissue turnover and maintenance. In the inflamed mucosa, butyrate stimulates regeneration at sites of the intestinal lining lesions. Moreover, experimental animal models of carcinogenesis have shown that butyrate can modify many metabolic actions and steps in the cell cycle, thereby counteracting early events in the cancer progression cascade and slowing progression [47]. In addition, an in vitro study indicated that butyrate inhibits tumor cell growth and proliferation by preventing their entry into the G1 phase of the cell cycle [48]. Nevertheless, RS3 prepared by different methods had different effects on SCFA production; specifically, PDYRS was more conducive to the generation of SCFAs. This was mainly caused by differences in the physicochemical properties and structures of the two RS3s. As described by Ma et al. [11], the chemical and structural characteristics of RS can influence the yield of total and individual SCFAs. Zhou et al. [49] speculated that the molecular structure of RS is one of the main factors affecting the yield and proportion of SCFAs. Gu et al. also showed that the fine molecular structure of RS3 affected SCFA production [50]. A recent study showed that even RSs with slight structural differences had different and highly specific effects on SCFA production by the gut microbiome [51].

The two types of RS3 analyzed in this study had noticeably different prebiotic properties. For example, PDYRS improved the relative abundance of Firmicutes and Bacteroidota and reduced the abundance of Proteobacteria, while ARYRS had the opposite effect. Certain Firmicutes in the intestine can ferment indigestible carbohydrates to produce SCFAs, which can promote host health. In particular, probiotic species such as butyric acid-producing Firmicutes bacteria have been found to increase the concentration of butyric acid in the colon, thereby improving intestinal function [52]. Furthermore, Bacteriodota express carbohydrate-active enzymes that can specifically degrade and utilize polysaccharide, thereby producing various SCFAs [53]. In addition, Bacteroidetes and Proteobacteria play an important role in the degradation of organic matter and in carbon cycling [54]. At the genus level, the relative abundance of the beneficial bacteria Bacteroides, Faecalibacterium, Blautia, unclassified_f_ Lachnospiraceae, Ruminococcus_torques_group, Eubacterium_eligens_group was increased, and the relative abundance of the harmful bacteria Escherichia-Shigella was decreased, by PDYRS.

Fermentation of ARYRS showed the opposite trend. Bacteroides can effectively improve mucosal angiogenesis, promote development of the immune system, and play an important role in maintaining the intestinal microecological balance [55, 56]. Blautia, Faecalibacterium, and Ruminococcus are good butyrate producers, and Ruminococcus is a key species in the human colon for degrading RS [57, 58]. Lachnospiraceae contains a large number of bacteria that produce high levels of butyrate [59], which could explain the high butyric acid production seen with PDYRS fermentation. Additionally, Eubacterium can stimulate butyric acid production through the butyryl-CoA:acetate CoA-transferase pathway [60]. A particularly interesting finding from out study was the distinct inhibitory effect of PDYRS on Escherichia and Shigella, which cause gastrointestinal disorders such as diarrhea [61]. Fermentation of ARYRS resulted in a lower relative abundance of Parasutterella compared with the blank control group. A variety of animal models and human studies have shown that Parasutterella abundance is negatively correlated with high-fat diet induced metabolic phenotypes (including hypothalamic inflammation) [40]. Taken together, our results suggest that supplementation with ARYRS and PDYRS changed the microbial composition of in vitro fecal fermentation cultures, and that these two RS3s had opposite effects on the gut microbiota, which may be related to the differences in their fine structures.

Conclusion

The present study shows that structural differences between yam RS3s may have substantial and distinct effects on SCFA production and overall gut microbiota composition. Fermentation of ARYRS and PDYRS increased the concentration of SCFAs, especially butyric acid; and PDYRS had the strongest effect in this regard. Both ARYRS and PDYRS can regulate the composition of intestinal flora, and PDYRS had a more beneficial prebiotic effect. PDYRS promoted the proliferation of beneficial bacteria such as Bacteroides, Faecalibacterium, Bautia, unclassified_f_ Lachnospiraceae, and inhibited Ruminococcus_torques_group, the growth Escherichia-Shigella conditional pathogens. Overall, the results from the present study suggest that pullulanase debranching is an effective method for producing yam RS3, and that PDYRS could be used to improve colon health and prevent related diseases by regulating fermentation metabolites and gut microbiota composition.

References

- Adebowale KO, Lawal OS. Effect of annealing and heat moisture conditioning on the physicochemical characteristics of Bambarra groundnut (*Voandzeia subterranea*) starch. *Nahrung Food.* 2002;46(5):311–316. https://doi.org/10.1016/s0308-8146(02)00100-0
- Augusto PED, Ibarz A, Cristianini M. Effect of high pressure homogenization (HPH) on the rheological properties of tomato juice: creep and recovery behaviours. Food Res Int. 2013;54(1):169–176.
 - https://doi.org/10.1016/j.foodres.2013.06.027
- Bhatnagar S, Hanna MA. Amylose-lipid complex formation during single-screw extrusion of various corn starches. *Cereal Chem.* 1994;71(6):582–587.
 - https://www.cerealsgrains.org/publications/cc/backissues/199 4/documents/71 582.pdf
- Amoako DB, Awika JM. Resistant starch formation through intrahelical V-complexes between polymeric proanthocyanidins and amylose. *Food Chem.* 2019;285:326–333. https://doi.org/10.1016/j.foodchem.2019.01.173
- Arijaje EO, Wang Y. Effects of enzymatic modifications and botanical source on starch-stearic acid complex formation. *Starch-Starke*. 2016;68:700–708. https://doi.org/10.1002/star.201500249
- Zou J, Xu M, Wen L, Yang B. Structure and physicochemical properties of native starch and resistant starch in Chinese yam

- (*Dioscorea opposita* Thunb.). *Carbohydr Polym.* 2020;237:116188. https://doi.org/10.1016/j.carbpol.2020.116188
- Yuan Y, Wang YB, Jiang Y, et al. Structure identification of a polysaccharide purified from *Lycium barbarium* fruit. *Int J Biol Macromol*. 2016;82:696–701.
 - https://doi.org/10.1016/j.ijbiomac.2015.10.069
- Liu G, Gu Z, Hong Y, Cheng L, Li C. Structure, functionality and applications of debranched starch: a review. *Trends Food Sci Technol.* 2017;63:70–79. https://doi.org/10.1016/j.tifs.2017.03.004
- Ashwar BA, Gani A, Shah A, Wani IA, Masoodi FA. Preparation, health benefits and applications of resistant starch – a review. *Starch-Starke*. 2016;68(3–4):287–301. https://doi.org/10.1002/star.201500064
- Doan HXN, Song Y, Lee S, Lee BH, Yoo SH. Characterization of rice starch gels reinforced with enzymatically-produced resistant starch. *Food Hydrocoll*. 2019;91:76–82. https://doi.org/10.1016/j.foodhyd.2019.01.014
- Ma Z, Boye JI. Research advances on structural characterization of resistant starch and its structure-physiological function relationship: a review. Crit Rev Food Sci Nutr. 2018;58(7):1059–1083. https://doi.org/10.1080/10408398.2016.1230537
- Recife ACD, Meneguin AB, Ferreira Cury BS, Evangelista RC. Evaluation of retrograded starch as excipient for controlled release matrix tablets. *J Drug Deliv Sci Technol.* 2017;40:83–94. https://doi.org/10.1016/j.jddst.2017.06.003
- Aparicio-Saguilan A, Flores-Huicochea E, Tovar J, Garcia-Suarez F, Gutierrez-Meraz F, Bello-Perez LA. Resistant starch-rich powders prepared by autoclaving of native and lintnerized banana starch: partial characterization. Starch-Starke. 2005;57(9):405–412. https://doi.org/10.1002/star.200400386
- Simsek S, El SN. Production of resistant starch from taro (Colocasia esculenta L. Schott) corm and determination of its effects on health by in vitro methods. Carbohydr Polym. 2012;90(3):1204–1209. https://doi.org/10.1016/j.carbpol.2012.06.039
- Jiang Q, Gao W, Shi Y, et al. Physicochemical properties and in vitro digestion of starches from different Dioscorea plants. Food Hydrocoll. 2013;32(2):432–439. https://doi.org/10.1016/j.foodhyd.2013.02.001
- Huang H, Jiang Q, Chen Y, et al. Preparation, physico-chemical characterization and biological activities of two modified starches from yam (*Dioscorea opposita* Thunb.). Food Hydrocoll. 2016;55:244–253.
 - https://doi.org/10.1016/j.foodhyd.2015.11.016
- 17. Jiang Q, Gao W, Li X, et al. Comparative susceptibilities to alkali-treatment of A-, B- and C-type starches of *Dioscorea zingiberensis*, *Dioscorea persimilis* and *Dioscorea opposita*. Food Hydrocoll. 2014;39:286–294.
 - https://doi.org/10.1016/j.foodhyd.2014.01.012
- American Association of Cereal Chemists (AACC). Approved Methods of Analysis, 2010.
- Nadiha MZN, Fazilah A, Bhat R, Karim AA. Comparative susceptibilities of sago, potato and corn starches to alkali treatment. Food Chem. 2010;121(4):1053–1059. https://doi.org/10.1016/j.foodchem.2010.01.048
- Association of Official Analytical Chemists (AOAC). Official Methods of The Association Official Analytical Chemists, 2002.
- Seong H, Bae JH, Seo JS, Kim SA, Kim TJ, Han NS. Comparative analysis of prebiotic effects of seaweed polysaccharides laminaran, porphyran, and ulvan using in vitro human fecal fermentation. *J Funct Foods.* 2019;57:408–416. https://doi.org/10.1016/j.jff.2019.04.014
- Zhou W, Yan Y, Mi J, et al. Simulated digestion and fermentation in vitro by human gut microbiota of polysaccharides from bee collected pollen of Chinese wolfberry. J Agric Food Chem. 2018;66(4):898–907.

- https://doi.org/10.1021/acs.jafc.7b05546.s001
- Gani A, Jan A, Shah A, et al. Physico-chemical, functional and structural properties of RS3/RS4 from kidney bean (*Phaseolus vulgaris*) cultivars. *Int J Biol Macromol.* 2016;87:514–521. https://doi.org/10.1016/j.ijbiomac.2016.03.017
- Zeng S, Wu X, Lin S, et al. Structural characteristics and physicochemical properties of lotus seed resistant starch prepared by different methods. *Food Chem.* 2015;186:213–222. https://doi.org/10.1016/j.foodchem.2015.03.143
- Ratnaningsih N, Suparmo, Harmayani E, Marsono Y. Physicochemical properties, in vitro starch digestibility, and estimated glycemic index of resistant starch from cowpea (*Vigna unguiculata*) starch by autoclaving-cooling cycles. *Int J Biol Macromol.* 2020;142:191–200. https://doi.org/10.1016/j.ijbiomac.2019.09.092
- Zhang Y, Zeng H, Wang Y, Zeng S, Zheng B. Structural characteristics and crystalline properties of lotus seed resistant starch and its prebiotic effects. *Food Chem.* 2014;155:311–318. https://doi.org/10.1016/j.foodchem.2014.01.036
- Wei C, Qin F, Zhou W, et al. Comparison of the crystalline properties and structural changes of starches from high-amylose transgenic rice and its wild type during heating. Food Chem. 2011;128(3):645–652. https://doi.org/10.1016/j.foodchem.2011.03.080
- Remya R, Jyothi AN, Sreekumar J. Effect of chemical modification with citric acid on the physicochemical properties and resistant starch formation in different starches. *Carbohydr Polym.* 2018;202:29–38. https://doi.org/10.1016/j.carbpol.2018.08.128
- Ji N, Li X, Qiu C, Li G, Sun Q, Xiong L. Effects of heat moisture treatment on the physicochemical properties of starch nanoparticles. *Carbohydr Polym.* 2015;117:605–609. https://doi.org/10.1016/j.carbpol.2014.10.005
- Flores-Morales A, Jimenez-Estrada M, Mora-Escobedo R. Determination of the structural changes by FT-IR, Raman, and CP/MAS C-13 NMR spectroscopy on retrograded starch of maize tortillas. Carbohydr Polym. 2012;87(1):61–68. https://doi.org/10.1016/j.carbpol.2011.07.011
- Li X, Gao X, Lu J, et al. Complex formation, physicochemical properties of different concentration of palmitic acid yam (*Dioscorea pposita* Thunb.) starch preparation mixtures. *Lwt Food Sci Technol.* 2019;101:130–137. https://doi.org/10.1016/j.lwt.2018.11.032
- Molavi H, Razavi SMA, Farhoosh R. Impact of hydrothermal modifications on the physicochemical, morphology, crystallinity, pasting and thermal properties of acorn starch. Food Chem. 2018;245:385–393. https://doi.org/10.1016/j.foodchem.2017.10.117
- Mao X, Lu J, Huang H, et al. Four types of winged yam (*Dioscorea alata* L.) resistant starches and their effects on ethanol-induced gastric injury in vivo. Food Hydrocoll. 2018;85:21–29. https://doi.org/10.1016/j.foodhyd.2018.06.036
- Birt DF, Boylston T, Hendrich S, et al. Resistant starch: promise for improving human health. *Adv Nutr.* 2013;4(6):587–601. https://doi.org/10.3945/an.113.004325
- Xie Z, Wang S, Wang Z, et al. In vitro fecal fermentation of propionylated high-amylose maize starch and its impact on gut microbiota. *Carbohydr Polym.* 2019;223:115069. https://doi.org/10.1016/j.carbpol.2019.115069
- Wu DT, Yuan Q, Guo H, et al. Dynamic changes of structural characteristics of snow chrysanthemum polysaccharides during in vitro digestion and fecal fermentation and related impacts on gut microbiota. *Food Res Int.* 2021;141:109888. https://doi.org/10.1016/j.foodres.2020.109888
- Zhang X, Aweya JJ, Huang ZX, et al. In vitro fermentation of Gracilaria lemaneiformis sulfated polysaccharides and its agaro-oligosaccharides by human fecal inocula and its impact on microbiota. Carbohydr Polym. 2020;234:115894.

- https://doi.org/10.1016/j.carbpol.2020.115894
- Wu DT, Nie XR, Gan RY, et al. In vitro digestion and fecal fermentation behaviors of a pectic polysaccharide from okra (*Abelmoschus esculentus*) and its impacts on human gut microbiota. *Food Hydrocoll.* 2021;114(3):106577. https://doi.org/10.1016/j.foodhyd.2020.106577
- Wu DT, Fu Y, Guo H, et al. In vitro simulated digestion and fecal fermentation of polysaccharides from loquat leaves: dynamic changes in physicochemical properties and impacts on human gut microbiota. *Int J Biol Macromol.* 2021;168:733–742. https://doi.org/10.1016/j.ijbiomac.2020.11.130
- Ju T, Kong JY, Stothard P, Willing BP. Defining the role of Parasutterella, a previously uncharacterized member of the core gut microbiota. ISME J. 2019;13(6):1520–1534. https://doi.org/10.1038/s41396-019-0364-5
- Reddy CK, Suriya M, Vidya PV, Haripriya S. Synthesis and physico-chemical characterization of modified starches from banana (Musa AAB) and its biological activities in diabetic rats. *Int J Biol Macromol.* 2017;94:500–507. https://doi.org/10.1016/j.ijbiomac.2016.10.050
- Reddy CK, Haripriya S, Mohamed AN, Suriya M. Preparation and characterization of resistant starch III from elephant foot yam (*Amorphophallus paeonifolius*) starch. Food Chem. 2014;155:38–44.
 https://doi.org/10.1016/j.foodchem.2014.01.023
- Zhang H, Jin Z. Preparation of products rich in resistant starch from maize starch by an enzymatic method. *Carbohydr Polym*. 2011;86(4):1610–1614. https://doi.org/10.1016/j.carbpol.2011.06.070
- Hoover R, Ratnayake WS. Starch characteristics of black bean, chick pea, lentil, navy bean and pinto bean cultivars grown in Canada. Food Chem. 2002;78(4):489–498. https://doi.org/10.1016/s0308-8146(02)00163-2
- Geirnaert A, Calatayud M, Grootaert C, et al. Butyrate-producing bacteria supplemented in vitro to Crohn's disease patient microbiota increased butyrate production and enhanced intestinal epithelial barrier integrity. *Sci Rep.* 2017;7(1):11450. https://doi.org/10.1038/s41598-017-11734-8
- Cummings JH, Englyst HN. Measurement of starch fermentation in the human large intestine. Can J Physiol Pharmacol. 1991;69(1):121–129. https://doi.org/10.1139/y91-018
- Brouns F, Kettlitz B, Arrigoni E. Resistant starch and "the butyrate revolution". Trends Food Sci Technol. 2002;13(8):251–261. https://doi.org/10.1016/s0924-2244(02)00131-0
- Sharma A, Yadav BS, Ritika. Resistant starch: physiological roles and food applications. *Food Rev Int.* 2008;24(2):193–234. https://doi.org/10.1080/87559120801926237
- Zhou Z, Cao X, Zhou JYH. Effect of resistant starch structure on short-chain fatty acids production by human gut microbiota fermentation in vitro. Starch-Starke. 2013;65(5–6):509–516. https://doi.org/10.1002/star.201200166
- Gu F, Li C, Hamaker BR, Gilbert RG, Zhang X. Fecal microbiota responses to rice RS3 are specific to amylose molecular structure. *Carbohydr Polym.* 2020;243:116475. https://doi.org/10.1016/j.carbpol.2020.116475
- Deehan EC, Yang C, Perez-Munoz ME, et al. Precision microbiome modulation with discrete dietary fiber structures directs short-chain fatty acid production. *Cell Host & Microbe*. 2020;27(3):389–404.e6.
 - https://doi.org/10.1016/j.chom.2020.01.006
- Xu SY, Aweya JJ, Li N, et al. Microbial catabolism of *Porphyra haitanensis* polysaccharides by human gut microbiota. *Food Chem.* 2019;289:177–186. https://doi.org/10.1016/j.foodchem.2019.03.050
- Thomas F, Hehemann JH, Rebuffet E, Czjzek M, Michel G. Environmental and gut bacteroidetes: the food connection.

- Front Microbiology. 2011;2:93. https://doi.org/10.3389/fmicb.2011.00093
- 54. Ma S, Fang C, Sun X, Han L, He X, Huang G. Bacterial community succession during pig manure and wheat straw aerobic composting covered with a semi-permeable membrane under slight positive pressure. *Bioresour Technol*. 2018;259:221–227.
 - https://doi.org/10.1016/j.biortech.2018.03.054
- Hooper LV. Bacterial contributions to mammalian gut development. *Trends Microbiol.* 2004;12(3):129–134. https://doi.org/10.1016/j.tim.2004.01.001
- 56. Stappenbeck TS, Hooper LV, Gordon JI. Developmental regulation of intestinal angiogenesis by indigenous microbes via Paneth cells. *Proc Natl Acad Sci USA*. 2002;99(24):15451–15455. https://doi.org/10.1073/pnas.202604299
- 57. Wang S, Zhang B, Chen T, Li C, Fu X, Huang Q. Chemical cross-linking controls in vitro fecal fermentation rate of high-amylose maize starches and regulates gut microbiota

- composition. *J Agric Food Chem.* 2019;67(49):13728–13736. https://doi.org/10.1021/acs.jafc.9b04410
- Perez-Burillo S, Hinojosa-Nogueira D, Pastoriza S, Rufian-Henares JA. Plant extracts as natural modulators of gut microbiota community structure and functionality. *Heliyon*. 2020;6(11):e05474. https://doi.org/10.1016/j.heliyon.2020.e05474
- Meehan CJ, Beiko RG. A phylogenomic view of ecological specialization in the *Lachnospiraceae*, a family of digestive tract-associated bacteria. *Genome Biol Evol.* 2014;6(3):703–713. https://doi.org/10.1093/gbe/evu050
- Louis P, Hold GL, Flint HJ. The gut microbiota, bacterial metabolites and colorectal cancer. Nat Rev Microbiol. 2014;12(10):661–672. https://doi.org/10.1038/nrmicro3344
- Verbeke KA, Boesmans L, Boets E. Modulating the microbiota in inflammatory bowel diseases: prebiotics, probiotics or faecal transplantation? *Proc Nutr Soc.* 2014;73(4):490–497. https://doi.org/10.1017/s0029665114000639